Numerical Predictions of Roughness Effects on the Performance Degradation of an Axial-Turbine Stage

Young-Seok Kang*
School of Mechanical and Aerospace Engineering, Seoul National University, Sin-Lim Dong, Gwan-Ak Gu, Seoul 151-742, Korea
Jae-Chun Yoo
Halla Climate Control Corp., Sinild dong, Daedeok Gu, Daejon 306-230, Korea
Shin-Hyoung Kang
Department of Mechanical and Aerospace Engineering, Seoul National University, Sin-Lim Dong, Gwan-Ak Gu, Seoul 151-742, Korea

This paper describes a numerical investigation on the performance deteriorations of a low speed, single-stage axial turbine due to use of rough blades. Numerical calculations have been carried out with a commercial CFD code, CFX-Tascflow, by using a modified wall function to implement rough surfaces on the stator vane and rotor blade. To assess the stage performance variations corresponding to 5 equivalent sand-grain roughness heights from a transitionally rough regime to a fully rough regime, stage work coefficient and total to static efficiency were chosen. Numerical results showed that both work coefficient and stage efficiency reduced as roughness height increased. Higher surface roughness induced higher blade loading both on the stator and rotor which in turn resulted in higher deviation angles and corresponding work coefficient reductions. Although, deviation angle changes were small, a simple sensitivity analysis suggested that their contributions on work coefficient reductions were substantial. Higher profile loss coefficients were predicted by higher roughness heights, especially on the suction surface of the stator and rotor. Furthermore sensitivity analysis similar to the above, suggested that additional profile loss generations due to roughness were accountable for efficiency reductions.

Key Words : Turbine, Roughness, Performance Degradation

Nomenclature

c : Speed
c_p : Pressure coefficient
k_s : Sand-grain roughness height
k^+ : Roughness Reynolds number
$\dot{m}$: Mass flow rate
p : Pressure
Q : Torque
Re : Reynolds number
s : Entropy
T : Temperature
U : Rotor tip speed
u^* : Friction velocity ($=\sqrt{\tau_w/\rho}$)
u^+ : Non-dimensional velocity
y^+ : Non-dimensional distance
α : Absolute flow angle
δ : Deviation angle
η : Efficiency

* Corresponding Author,
E-mail : electra@turbo.snu.ac.kr
TEL : +82-2-880-7118; **FAX** : +82-2-883-1215
School of Mechanical and Aerospace Engineering, Seoul National University, Sin-Lim Dong, Gwan-Ak Gu, Seoul 151-742, Korea. (Manuscript **Received** November 23, 2005; **Revised** March 31, 2006)

ν : Kinematic viscosity
ϕ : Flow coefficient
ρ : Density
ξ : Loss coefficient
ψ : Work coefficient
ω : Rotating speed

Superscripts
$*$: Smooth case
$**$: One dimensional

Subscripts
abs : Absolute value
rel : Relative value
1 : Stator inlet
2 : Stator outlet (rotor inlet)
3 : Rotor outlet
s : Static condition
t : Total condition

1. Introduction

Blade surfaces in the turbine stage experience significant performance degradation during operation. Deposition of foreign dust, thermal erosion, collision or pitting of particles, result in increase of surface roughness of stator or rotor blades and such a grown surface roughness adversely affects stage performance such as stage efficiency, work coefficient, or rate of heat transfer. Many previous experimental studies have focused on these performance deteriorations. Bammert et al.(1980) reported that rough surfaced cascade blades promote transition to turbulent flow and increase friction coefficients, which result in a efficiency drop of 7~14 percent. In addition, Boyton et al. (1993) tested a fully setup system and found that stage efficiency improves by 2 percent when the rough coating of turbine rotor blades is polished. Consequently, surface roughness causes substantial deterioration of turbine stage efficiency. Bammert et al.(1980) also reported that increase in profile loss due to roughness at the suction side was 2~3 times higher than that of the pressure side. Kind et al.(1998) differentiated the roughness effect on different locations of the rotor and stator in a turbine cascade and found that roughness on the suction surface caused substantial increase in profile loss compared to the pressure surface. Most of these researches were carried out by experimentation. However, experimenting with surface roughness is known to be difficult to execute and more database for turbine performance is required.

Therefore, numerical investigation on the roughness effect has also been initiated recently. Kind et al.(1998) also carried out inviscid calculations using a vortex panel method with source distributions to represent boundary layer displacement effect, and results coincided with their measured data. Guo et al.(1998) used a three-dimensional CFD code to predict local Mach number and heat transfer coefficients over airfoil surfaces and end-walls of a transonic gas-turbine nozzle guide vane. They modified the law of the wall for calculations on rough surfaces and their results conformed to the overall trend of the measured data. Boyle et al.(2003) also tried a numerical method with a quasi-3D Navier-Stokes code for a rough linear turbine cascade and showed the relationship between the profile loss and the Reynolds number. Most recently, Shabbir et al.(2004) modified Spalding's formula to predict skin friction of rough surface and validated their code by comparing their results with measured rough cascade data by Bammert et al.(1972). Recently, some commercial CFD codes such as TASCflow, Flow 3D have appended capabilities for rough surfaces by modifying the law of the wall (AEA-Technology, 1999; Souders et al., 2002).

However, most of the precedent studies regarding roughness effects have been carried out with a cascade. Few researches regarding roughness effects on a fully rotating system have been reported and few measured data is available. Therefore we simulated flows in a low speed, single-stage axial flow turbine stage with and without roughness on the stator and rotor surfaces to predict performance deterioration. Themain objective of this study is to estimate amounts of performance deterioration due to change in surface roughness on the stator and rotor and investigate the main source of roughness effect on performance reduction.

2. Roughness Modeling in CFD

It is well known that surface roughness has little influence on the velocity profiles in a laminar flow. But in a turbulent flow, even a small amount of roughness will break up the thin viscous inner layer and greatly increase wall friction and momentum and heat transfers (White, 1991). The logarithmic overlap layer begins to deviate from that of the smooth wall by amount of Δu^+ as appeared in Eq. (1). The Δu^+ is usually modeled as a function of the roughness Reynolds number, k^+ defined in Eqs. (2) and (3).

$$u^+=\frac{1}{0.41}\ln y^+ +5.0-\Delta u^+ \tag{1}$$

$$\Delta u^+=\frac{1}{0.41}\ln(1+0.3k^+) \tag{2}$$

$$k^+=\frac{k_s u^*}{v} \tag{3}$$

There are three roughness regimes corresponding to k^+ (Nikuradse, 1933).

$k^+<5$: hydraulically smooth wall
$5<k^+<70$: transitional-roughness regime
$k^+>70$: fully rough flow

The main idea of implementing roughness effects into TASCflow is to use a modified wall function, e.g. Eq. (1), instead of the conventional one (AEA Technology, 1999). Some precedent researches showed this simple modification could reasonably predict the velocity profile (Souders et al., 2002) and friction coefficient near the rough wall (Kang et al., 2003). Due to this effectiveness, many commercial CFD codes adopt this type of roughness modeling. It should be noted that turbulence transition cannot be predicted with this modeling. However turbulence transition occurs at the fore part of the blade (Yun et al., 2004) and early transition has little effects on the main flow. Therefore transition effects were not taken into account into this calculation. In this study, CFX-TASCflow is used for numerical analysis for a turbine stage with rough stator and rotor blades.

3. Validation of Roughness Modeling

The roughness modeling in TASCflow is assessed by comparing the numerical results of a rough NACA 65-0610 airfoil with available measured data by Bammert (1972). Fig. 1 shows computational grid of the airfoil. To match the experimental condition, stagger angle and flow angle are set to be 48 deg and 52.5 deg, respectively. Solidity is set to be 1.0. Inlet total pressure, which is given as the inlet boundary condition with flow angle, is evaluated from the Reynolds number of 4.3×10^5. Also static pressure condition is specified at the outlet boundary condition. Five different normalized roughness heights, $k_s/l=0.23\times10^{-3}$, 0.56×10^{-3}, 1.56×10^{-3}, 3.22×10^{-3} and 5.56×10^{-3} are given to simulate roughness effects.

Figures 2 and 3 show distributions of mass averaged loss coefficient and turning angle at the exit of the airfoil. The result show that as the roughness height increases, both loss and deviation angle increase. Higher total pressure loss region appears at the trailing edge of the suction surface while the pressure surface scarcely affected, which is not presented in this paper. As a result, higher pressure difference between the pressure and suction sides occurs at the trailing edge and it leads to a less turning of the working fluid. Similar calculations were carried out by Shabbir et al.(2004). They also tried to predict roughness effects by modifying wall function with

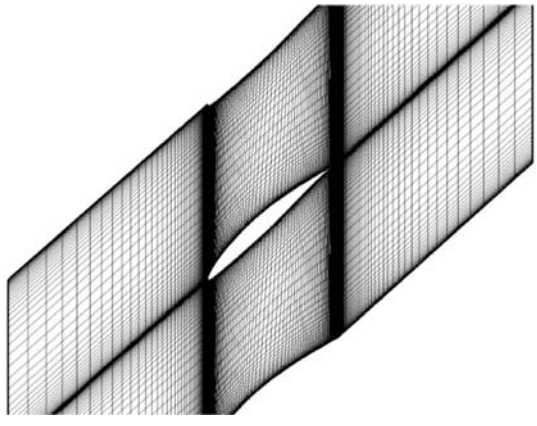

Fig. 1 Computational grid of NACA 65-1210

Spalding's formula and similar trend appeared both in the turning angle and loss coefficient distributions. Both results show that when the roughness height is high enough to be in the fully rough regime (in this study, when k_s/l is over 3.22×10^{-3}), their change ratios of loss and turning angle become less sensitive to the surface roughness. Comparing our calculation results with Bammert's experimental results and Shabbir's numerical results, it can be said that roughness modeling in TASCflow reasonably predicted the roughness effects.

Although both results show the correct trends for loss and deviation, the experimental data show a more pronounced roughness effect. The major reason of these differences is that numerical results do not predict flow separation near the trailing edge that appeared in the experimental results (Bammert, 1973). But prediction of separation is sensitive to turbulence modeling, Reynolds number and so on. Therefore the current roughness modeling is not fully responsible for the underestimated results. And also Shabbir (2003) pointed out that the aspect ratio of the experimental cascade is not sufficiently high enough to avoid three dimensional effects and the cascade with 4 passages is not necessarily periodic.

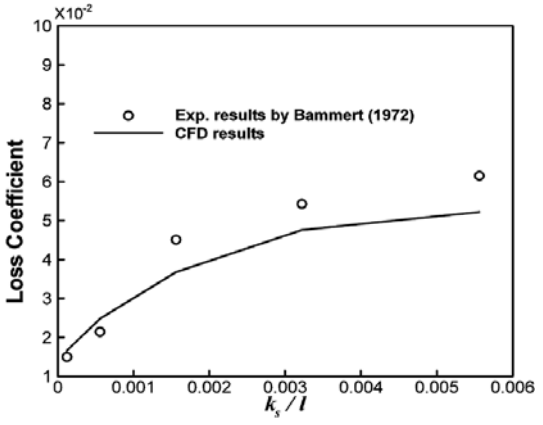

Fig. 2 Distributions of loss coefficients

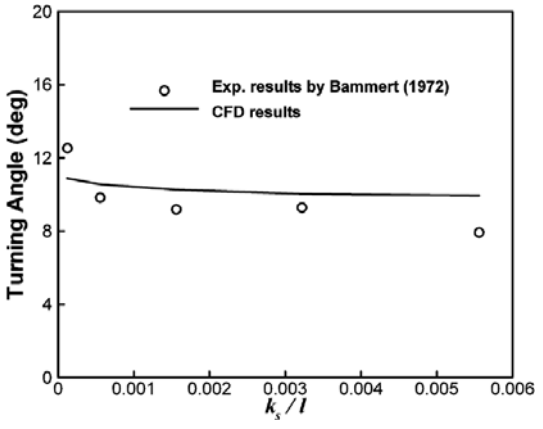

Fig. 3 Distributions of turnina anales

4. Numerical Simulations of an Axial Turbine Stage

Table 1 gives brief specifications of an axial turbine stage for this study. The turbine stage was designed and experimented by Yoon (2002). The maximum rotating speed is 1600 rpm and the maximum shaft power is 15 kW. At the design point, the inlet flow velocity is 20 m/s.

Steady state calculations have been carried out with a commercial CFD code, CFX-TASCflow, which is a FVM based solver for the Navier-Stokes equation using a flexible multi-block grid system and several sophisticated modeling tools, especially for rotating machinery and combustion applications. To support parallel computation capability of TASCflow, a cluster computer with 8 AMD MP 2400+ CPUs was used. Approximately 3 hours were taken to get a converged solution for each case. The maximum residual convergence criterion for mass and momentum equations was set to be 10^{-5}.

Figure 4 shows computational grids comprised

Table 1 Specification of turbine stage

	Stator	Rotor
Axial chord [mm]	96.01	41.04
Hub diameter [mm]	562.8	560.0
Tip diameter [mm]	700.0	697.2
Number of vanes/blades	38	70
Solidity	1.87	1.53
Inlet angle [deg]	0	62.3
Exit angle [deg]	77.3	74.6
Re. based on chord	4.1×10^5	2.2×10^5

of one stator vane and two rotor blades. Tip clearances are not considered. Both the stator and rotor domains consist of 5 grid blocks, respectively. The number of total grids is approximately 600,000.

There are some suggestions for near-wall grid spacing when the wall is rough. Wilcox (1993) suggested using a relatively large grid element size adjacent to a boundary. "Large" means covering the region of rapid variation in turbulence variables and relying on the wall function to set the proper average values in this region. TASCflow also suggests a similar near-wall grid spacing method for the rough wall (AEA-Technology, 1999). For this reason, great care was taken to construct near wall grid structure. In this study, the first grid size near the wall is set to be an order of the roughness height (approximately 0.1 mm) to satisfy the y^+ value at the first grid from the wall to be between 11 and 20.

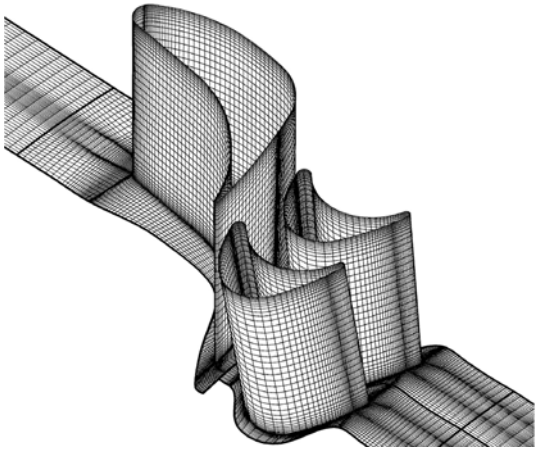

Fig. 4 Computational grid of an axial turbine stage

For the boundary conditions, total pressure and total temperature at the operating condition were specified at the inlet and mass flow rate was specified for the outlet boundary condition. The frozen-rotor method was used for the interface treatment between the stator and rotor stages. The frozen-rotor method is generally dependent on a relative position of the stator and rotor, several

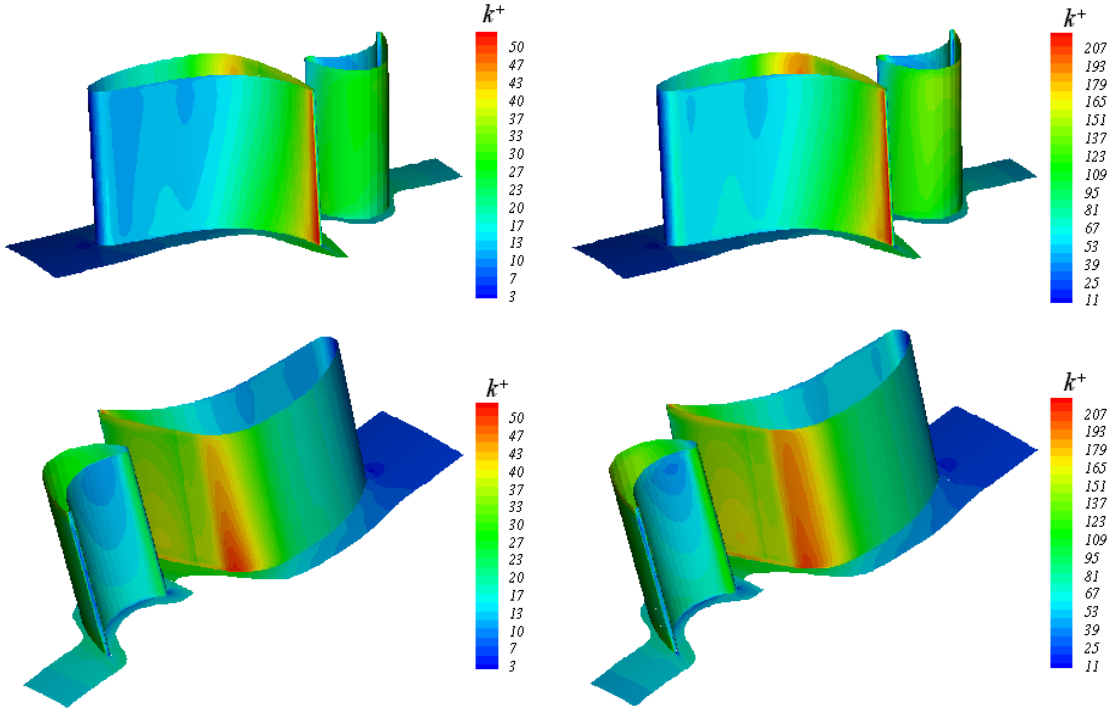

(a) (b)

Fig. 5 Roughness Reynolds number distributions (a) k_s=106 μm and (b) k_s=400 μm

calculations have been carried out and we found that relative positions have little influence on the result. The high Reynolds k-ω turbulence model was used with the turbulence intensity of 5% and the eddy viscosity ratio to fluid viscosity of 10 at the inlet.

In TASCflow, equivalent sand-grain roughness height option is available for the rough wall boundary condition. 5 roughness heights were used in this study, k_s=0 (smooth), 106 μm and 156 μm for the transitionally rough regimes, 236 μm and 400 μm for the fully rough regimes. See Yun et al. (2004) for evaluation of roughness heights for each roughness regime. In this study, to differentiate an individual roughness effect of the stator and the rotor, three different calculations were carried out for each roughness height ; roughness only on the stator surface, only on the rotor surface and on both the stator and rotor surfaces. Fig. 5 Shows distributions of roughness Reynolds number, evaluated from Eq. (3) for the case of (a) k_s=106 μm and (b) k_s=400 μm roughness height on the stator and rotor surface. When k_s= 106 μm, the overall roughness Reynolds number is less than 70 which is transitionally rough regime. Also for the k_s=400 μm, the overall roughness Reynolds number is beyond 70 and it is in the fully rough regime. It confirms that roughness height on the stator and rotor and spacing first grid are reasonably given.

5. Results and Discussions

5.1 Distributions of work coefficients and pressure coefficients

Stage work coefficient, ψ is define as follows.

$$\psi=\frac{Q\omega}{\dot{m}U^2} \tag{1}$$

Torque is evaluated by integrating multiplication of shear and pressure forces acting on the solid wall and their corresponding position. The turbine Euler equation shows that the value of torque is equivalent to the total enthalpy transfer across the rotor stage. Fig. 6 shows relative changes of the work coefficients corresponding to the roughness heights. There are two regions on x-axis corresponding to the roughness Reynolds number. As the roughness height increases, the amount of work reduction also increases. Also it can be seen that roughness on the stator surface is more influential and more sensitive to the work reduction. Work reduction due to the rough stator is approximately much higher than that of the rough rotor. It is also found that sum of work reduction due to the rough stator (dashed line) and that of the rough rotor (dash-dot line) is approximately equivalent to that of both the stator and rotor roughened (solid line). As the work coefficient is associated with blade loading and flow angle, Figs. 7 and 8 show distributions of pressure coefficients at the mid-span of the stator and rotor. Eqs. (5) and (6) define the pressure coefficient of

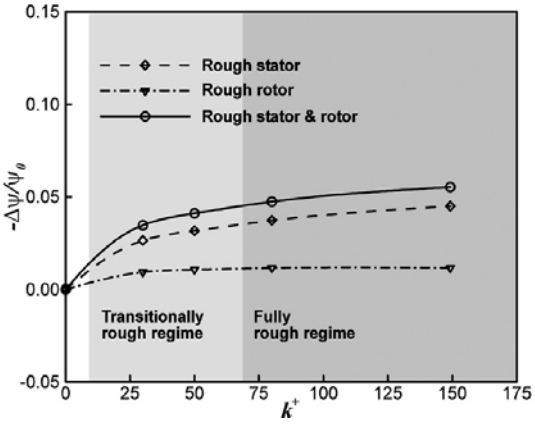

Fig. 6 Distributions of work coefficient reductions

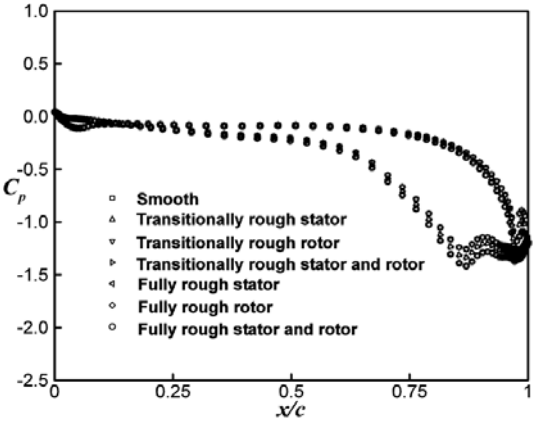

Fig. 7 Distributions of pressure coefficient at the mid-span of the stator

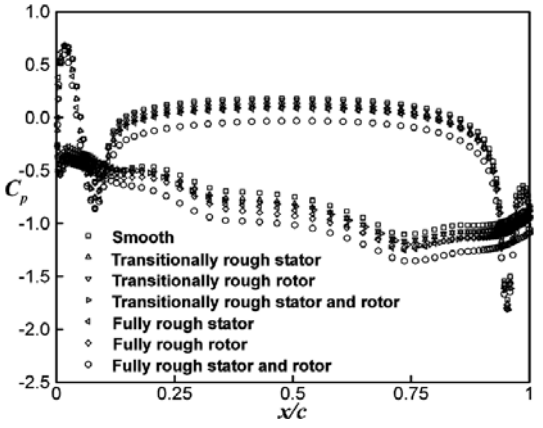

Fig. 8 Distributions of pressure coefficient at the mid-span of the rotor

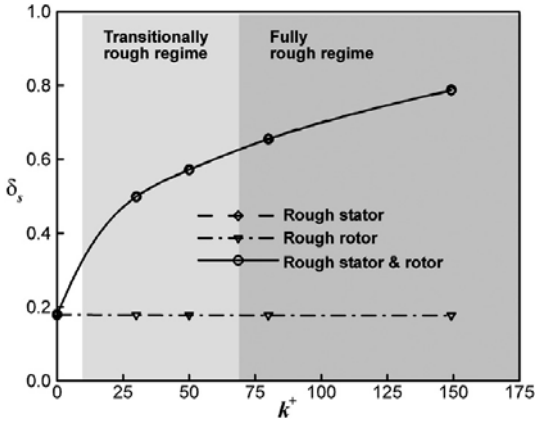

Fig. 9 Distributions of deviation angle of the stator

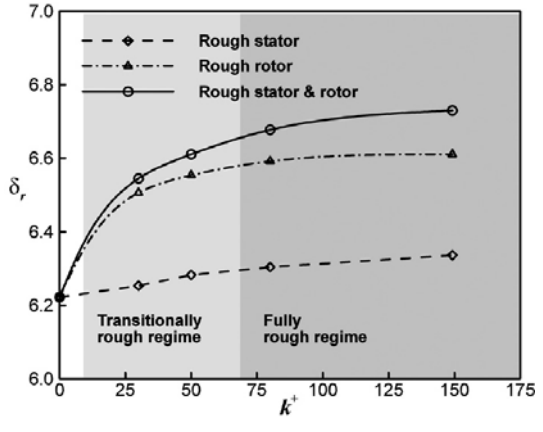

Fig. 10 Distributions of deviation angle of the rotor

the stator and rotor respectively. Also Figs. 9 and 10 show deviation angles of the stator and rotor.

$$c_{p,s}=\frac{p-p_1}{p_{t2,abs}-p_{s2}} \tag{5}$$

$$c_{p,r}=\frac{p-p_2}{p_{t3,rel}-p_{s3}} \tag{6}$$

In Fig. 7, there are little changes at the pressure surface of the stator. However, noticeable changes appear near the trailing edge of the suction surface. Higher roughness decreases the pressure coefficient at the suction surface. This causes higher pressure difference between the pressure and suction sides near the trailing edge which induces higher deviation angle of the stator as shown in Fig. 9. This result well agrees with the results of some previous studies (Kind et al., 1998 ; Guo et al., 1998). Their results showed that total pressure loss highly increases especially at the suction surface and it affects corresponding pressure coefficient. Similar trend appears in the pressure coefficients on the rotor surface. It is somewhat complicated because of upstream effects. But as of the stator pressure coefficients, roughness on the rotor surface decreases the static pressure at the suction surface while that of the pressure surface is scarcely affected. In a similar manner, pressure difference between two sides at the rotor gradually increases as the roughness height increases and it also results in a higher deviation angle of the rotor. It is interesting that deviation angle of the rotor gradually increases as the roughness height on the stator surface increases. It is caused by change in the upstream flow angle at the stator outlet. Its contribution will be discussed in the following one-dimensional analysis. These roughness effects on the deviation angle changes are schematically illustrated in Fig. 11.

As mentioned before, the roughness effects on the pressure coefficients and corresponding deviation angle changes are small. Nevertheless, their effects on the work coefficient of the turbine stage are quite considerable. Therefore, following simple sensitivity analysis is described to quantify the deviation angle effects on the work coefficient. The well known Euler turbine equation with a velocity triangle in Fig. 11 gives a following equation.

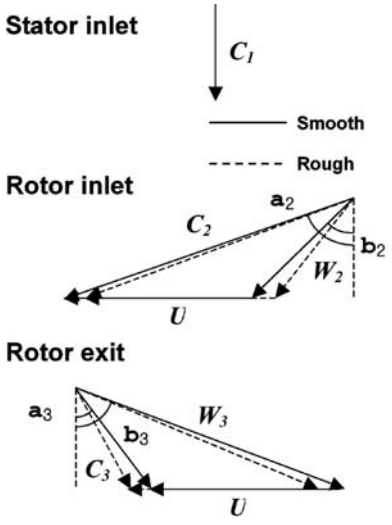

Fig. 11 Schematic velocity triangle changes due to roughness

$$\psi=\phi(\tan\alpha_2-\tan\beta_3)-1 \tag{7}$$

Differential form of the Eq. (7) is

$$d\psi=(\tan\alpha_2-\tan\beta_3)\,\delta\phi - \phi\sec^2\alpha_2 d\delta_s-\phi\sec^2\beta_3 d\delta_r \tag{8}$$

Also from the velocity triangle, following relations are derived.

$$d\alpha_2=-d\delta_s,\ d\beta_3=d\delta_r \tag{9}$$

Substitution Eq. (9) into Eq. (8) and neglecting the flow coefficient perturbation term leads to the following equation.

$$\delta\psi=\phi\sec^2\alpha_2 d\delta_s-\phi\sec^2\beta_3 d\delta_r \tag{10}$$

For infinitesimal changes, Eq. (10) can be written as follows.

$$\Delta\psi^{**}=-\phi^*\sec^2\alpha_2^*\Delta\delta_s-\phi^*\sec^2\beta_3^*\Delta\delta_r \tag{11}$$

Where $\Delta\delta_s=\delta_s-\delta_s^*$ and $\Delta\delta_r=\delta_r-\delta_r^*$. These incremental terms are evaluated with area averaged values. Eq. (11) shows that reduction of the work coefficient is proportional to the changes in the deviation angles.

Table 2 shows contributions of these two terms to the reduction of the work coefficient. Summations of these two terms are approximately equivalent to the actual work coefficient reductions in Fig. 6. Therefore, it can be said that this sensitivity analysis reasonably predicts contributions of these two terms to the reduction of the work coefficient. Table 2 shows that the transitionally rough (k_s=106 μm) and fully rough stator (k_s=400 μm) decreases the work coefficient by 3.1% and 5.9%, respectively. Influence of the rough rotor is smaller than that of the rough stator. The transitionally rough and fully rough rotor decreases the work coefficient by 0.9 and 1.3%, respectively. The higher exit flow angle of the stator makes the stator deviation angle more sensitive to the work coefficient reduction. And a summation of the work coefficient reductions of the rough stator and rough rotor is approximately equivalent to that of totally roughened stage. For k_s=106 μm, the work reduction of the totally roughened stage is approximately 4.2% and it is 7.6% for k_s=400 μm.

Table 2 Sensitivity analysis of work coefficient reductions

	k^2 (height)	$\frac{\Delta\psi\delta_s}{\psi^*}$	$\frac{\Delta\psi\delta_r}{\psi^*}$	$\frac{\Delta\psi^{**}}{\psi^*}$	$\frac{\Delta\psi}{\psi^*}$
Stator	30 (106 μm)	−0.031	−0.001	−0.032	−0.027
Rotor		0.000	−0.009	−0.009	−0.009
All		−0.031	−0.010	−0.042	−0.035
Stator	50 (156 μm)	−0.038	−0.002	−0.040	−0.032
Rotor		0.000	−0.011	−0.011	−0.011
All		−0.038	−0.012	−0.050	−0.041
Stator	80 (236 μm)	−0.047	−0.003	−0.050	−0.037
Rotor		0.000	−0.012	−0.012	−0.012
All		−0.047	−0.015	−0.061	−0.047
Stator	149 (400 μm)	−0.059	−0.004	−0.063	−0.045
Rotor		0.000	−0.013	−0.013	−0.012
All		−0.060	−0.016	−0.076	−0.055

Even though there are small changes in the deviation angles due to the roughness, this sensitivity analysis shows that their effects on the work coefficient are significant. The rate of the work coefficient reduction decreases as the roughness height increases. Because, as mentioned before, the rate of increase in the deviation angle decreases as the roughness height increases.

5.2 Distributions of efficiency and loss coefficient

Total to static efficiency is defined as follows,

$$\eta=\frac{Q\omega}{\dot{m}c_p T_{t1}\left(1-(p_{s3}/p_{t1})^{\frac{\gamma-1}{\gamma}}\right)} \tag{12}$$

Figure 12 shows distributions of the efficiency reductions corresponding to roughness Reynolds number. As of the work reductions, the roughness on the stator surface has a more contribution to the efficiency reductions. Efficiency reductions are more sensitive in the transitionally rough regime. In the fully rough regime, the efficiency reduction slope becomes gentler. The efficiency reduction due to the rough stator is approximately two times higher than that of the rough rotor for all roughness Reynolds numbers and their sum is approximately equivalent to that of the totally rough stage. It is well known that surface roughness thickens boundary layer and promotes transition to the turbulent flow. Therefore investigation of the total pressure loss coefficients is required to account for the efficiency reduction. Eqs. (13) and (14) defines the loss coefficients of the stator and rotor respectively.

$$\xi_s=\frac{p_{t1,abs}-p_{t2,abs}}{p_{t1,abs}-p_{s3}} \tag{13}$$

$$\xi_r=\frac{p_{t2,rel}-p_{t3,rel}}{p_{t1,abs}-p_{s3}} \tag{14}$$

Figure 13 shows distributions of the loss coefficients of the stator. As the roughness height of the stator increases, the loss coefficient also increases. In Fig. 9, as deviation angle of the stator slightly changes as the rotor roughness increases, incidence loss at the following rotor row decreases. As a result, the rough rotor slightly reduces the loss coefficients of the stator. The loss coefficients at the rotor outlet show a similar trend in Fig. 14. Roughness of the rotor surface is the main source of the loss generation in the rotor stage. Comparing Figs. 13 and 14, the amount of loss generation in the stator is approximately 20% higher than that of the rotor. It is interesting that the stator roughness hardly contributes to the rotor loss generations.

For each roughness height, summations of additional loss of the rough stator and the rough rotor are approximately equivalent to that of the totally roughened stage. As shown in Fig. 12, the variations of efficiency shows similar trend with that of the loss coefficient. A summation of the

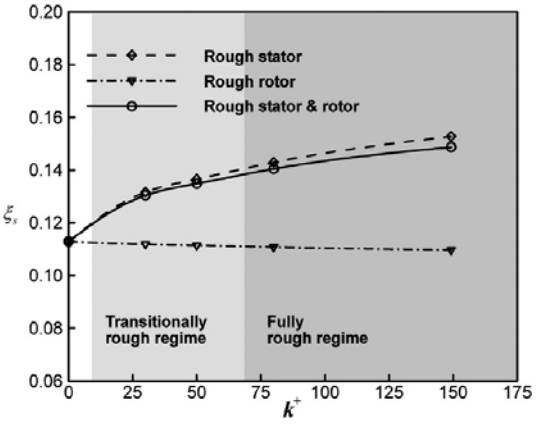

Fig. 13 Distributions of loss coefficient of the stator

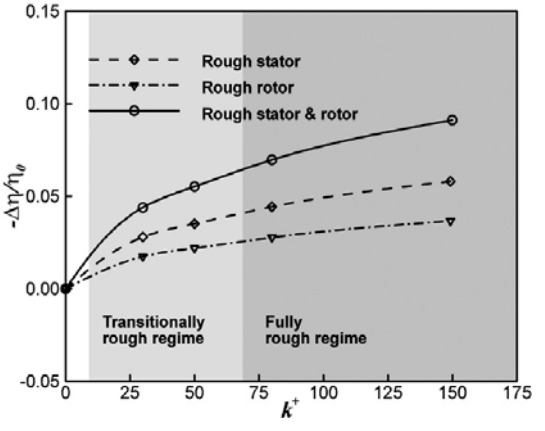

Fig. 12 Distributions of efficiency reductions

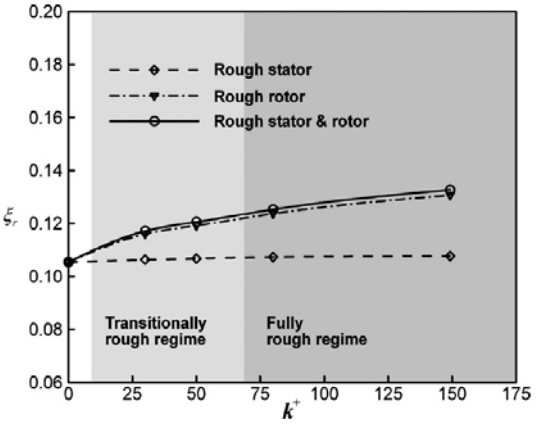

Fig. 14 Distributions of loss coefficient of the rotor

Table 3 Sensitivity analysis of efficiency reductions

	k^+ (height)	$\frac{\Delta\eta_{\xi_s}}{\eta^*}$	$\frac{\Delta\eta_{\xi_r}}{\eta^*}$	$\frac{\Delta\eta_{\xi_s}}{\eta^*}$	$\frac{\Delta\eta_{\xi_r}}{\eta^*}$	$\frac{\Delta\eta^{**}}{\eta^*}$	$\frac{\Delta\eta}{\eta^*}$
Stator	30 (106 μm)	−0.025	−0.001	−0.001	0.000	−0.027	−0.028
Rotor		0.001	−0.015	0.000	−0.001	−0.015	−0.017
All		−0.024	−0.016	−0.001	−0.001	−0.042	−0.044
Stator	50 (156 μm)	−0.032	−0.002	−0.002	0.000	−0.036	−0.035
Rotor		0.002	−0.019	0.000	−0.001	−0.018	−0.022
All		−0.030	−0.021	−0.002	−0.001	−0.054	−0.055
Stator	80 (236 μm)	−0.041	−0.003	−0.002	0.000	−0.046	−0.044
Rotor		0.003	−0.025	0.000	−0.001	−0.023	−0.028
All		−0.037	−0.027	−0.002	−0.001	−0.068	−0.070
Stator	149 (400 μm)	−0.054	−0.003	−0.002	0.000	−0.059	−0.058
Rotor		0.004	−0.034	0.000	−0.002	−0.032	−0.037
All		−0.049	−0.037	−0.002	−0.002	−0.090	−0.091

efficiency drop of the rough stator and that of the rough rotor is almost the same with that of totally roughened stage.

Similar sensitivity analysis has been carried out to quantify contributions of loss coefficients to the efficiency reduction. The total to static efficiency can be redefined with suggested loss coefficients as follows.

$$\eta_{t-s}=\frac{2\phi(1-\xi_s-\xi_r)(\tan\alpha_2-\tan\beta_3)-1}{\phi^2\sec^2\beta_3+2\tan\alpha_2-1} \quad (15)$$

The linearized form of Eq. (15) for the infinitesimal changes is Eq. (16)

$$\Delta\eta_{t-s}=-2\frac{A}{B}\Delta\xi_s-2\frac{A}{B}\Delta\xi_r - \frac{2\phi\sec^2\alpha_2 C(B-2A)}{B^2}\Delta\delta_s - \frac{2\phi\sec^2\beta_3 C(\beta+2\phi\tan\beta_3 A)}{B^2}\Delta\delta_r \quad (16)$$

where $A=\phi(\tan\alpha_2-\tan\beta_3)-1$, $B=\phi^2=\sec^2\beta_3+2\phi\tan\alpha_2-1$, $C=(1-\xi_s-\xi_r)$.

The first two terms of the right-hand side of Eq. (17) are contributions of the loss coefficient and next two terms are those of the deviation angle changes. Table 3 summarizes these effects on the efficiency reductions. It reveals clearly that the dominant source of the efficiency reduction is the additional loss generations. In the previous

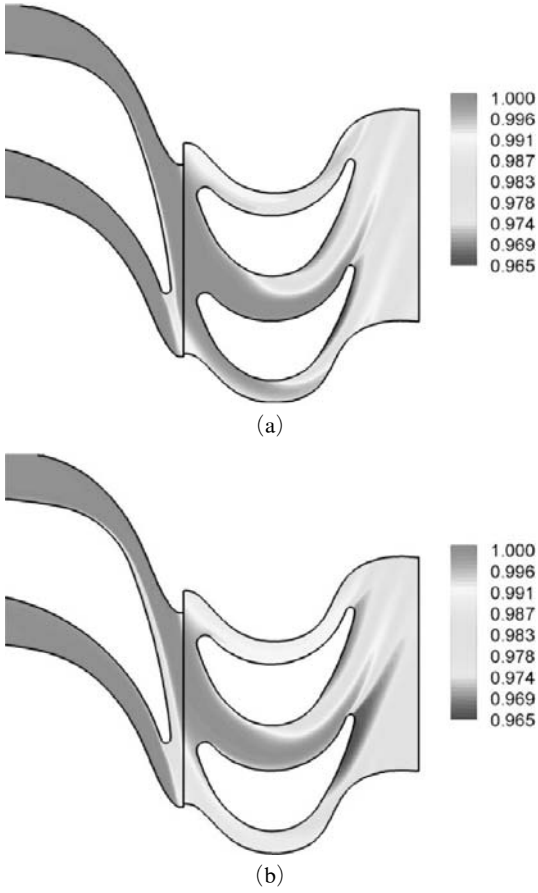

Fig. 15 Distributions of normalized entropy at the mid-span of (a) smooth and (b) fully rough (k_s=400 μm) stage

section, as shown in Table 2, although deviation angle changes are dominant source of the work reduction, they have negligible effects on the efficiency reductions. It shows that summation of the efficiency reductions of the rough stator and rough rotor approximately equals the efficiency reduction of the totally rough stage. And it also shows that summation of these four discrete terms is almost equivalent to the actual efficiency reduction indicated in the last column.

Figure 15 illustrates normalized entropy defined in Eqs. (17) and (18) at the mid-span which shows loss distributions in the stator and rotor stages at a time.

$$\Delta s = c_p \ln\left(\frac{T_t}{T_{t1}}\right) - R \ln\left(\frac{p_t}{p_{t1}}\right) \tag{17}$$

$$\xi = \exp(-\Delta s/R) \tag{18}$$

This figure shows that most of the additional loss comes from the profile loss generated in the boundary layer. At the rough stator stage, large amount of loss is generated near the trailing edge of the stator suction surface compared to the smooth stator stage. For this reason, the wake region occupies a large portion of the flow field near the rough stator outlet. Moreover, the additional profile loss generated in the stator flows downstream. Comparing the rotor with the rough stator to that of the smooth stator, ξ even in the core flow of the rotor with the rough stator has lower value (higher loss). Likewise, in the rotor stage, large amount of profile loss is generated near the trailing edge of the suction surface and the wake region propagates farther before mixing with the core flow.

6. Conclusions

Numerical calculations of through flows for a low speed, single stage axial turbine with different roughness have been carried out. The conclusions from these calculations are as follows.

(1) Roughness on the blade surfaces does not have severe effects on the blade surface pressure distribution and corresponding deviation angle changes of the stator and rotor. However, one dimensional sensitivity analysis suggested that small changes in deviation angles have significant effects on the stage work coefficient. It should be noted that even though change in the deviation angle of the rough stator is smaller than that of the rough rotor, its influence on the work coefficient is higher than that of the rough rotor.

(2) Work coefficient reductions of the rough stator and rough rotor are separated corresponding to location of the surface roughness. Their summations equal the work reduction of the totally rough stage for each roughness height.

(3) Blade surface roughness severely deteriorates stage efficiency. Additional loss due to surface roughness is the dominant term that reduces stage efficiency. An entropy contour shows that most of the additional loss resulted from increased profile loss which is due to thickened boundary layers.

(4) Summation of drops in efficiency level of the rough stator and rough rotor approximately equals that of the totally rough stage. Similar trends appear in the loss distribution. It is evidence that additional loss generation is the most influential over efficiency reduction.

Acknowledgments

This work was supported by the Brain Korea 21 Project in 2005.

References

AEA-Technology, 1999, "CFX-TASCflow Theory Documentation version 2.9".

Bammert, K. and Sandstede, H., 1980, "Measurements of the Boundary Layer Development along a Turbine blade with Rough Surface," *ASME J. Turbomach.*, 102, pp. 978～983.

Bammert, K. and Milsch, R., 1972, "Boundary Layers on Rough Compressor Blades," ASME Paper No. 72-GT-48.

Boyle, R. L. and Senyitko, R. G., 2003, "Measurements and Prediction of Surface Roughness Effects on Turbine Vane Aerodynamics," ASME paper GT2003-38580

Boynton, J. L., Tabizadeh, R. and Hudson, S. T, 1993, "Investigation of Rotor Blade Roughness

Effects on Turbine Performance," *ASME J. Turbomach.*, 124, pp. 614～620.

David, C. Wilcox, 1993, "Turbulence Modeling for CFD," DCW Industries, Inc.

Frank M. White, 1991, "Viscous Fluid Flow," McGraw Hill.

Guo, S. M., Jones, T. V., Lock, G. D. and Dancer, S. N., 1998, "Computational Prediction of Heat Transfer to Gas Turbine Nozzle Guide Vanes With Roughened Surfaces," *ASME J. Turbomach.*, 120, pp. 343～350.

Kang, S. H., Kang, Y. S. and Han, K. H., 2003, "Numerical Study on Blade Roughness Effect on the Performance of Turbo-machines," IGTC2003-TS033.

Kind, R. J., Serjak, P. J., Abbott, M. W. P., 1998, "Measurments and Prediciton of the Effects of Surface Roughness on Profile Losses and Deviation in a Turbine Cascade," *ASME J. Turbomach.*, 120, pp. 20～27.

Nikuradse, J., 1933, "Laws For Flows In Rough Pipes," *VDI-Forchungsheft 361*, Series B, Vol. 4, pp. 361.

Schlichting, H., 1979, "Boundary Layer Theory," 7th Edition, McGraw-Hill, New York.

Souders, D. T. and Hirt, C. W., 2002, "Modeling Roughness Effects in Open Channel Flows," Flow Science Technical Note (FSI-02-TN60).

Yoon, Y. S., 2002, "Turbine Experiment Equipment Design and Blades Performance Evaluation," M.S Thesis, Seoul National University.

Yun, Y. I., Park, I. Y. and Song, S. J., 2004, "Performance Degradation Due to Blade Surface Roughness in a Single-Stage Axial Turbine," ASME Papers 2004-GT-53094.